Molecular Drivers of Aging in Biomolecular Condensates: Desolvation, Rigidification, and Sticker Lifetimes

Subhadip Biswas, Davit A Potoyan
Department of Chemistry
Iowa State University
Email: subhadip@iastate.edu

Motivation

Biomolecular condensates are crucial for various cellular functions due to their dynamic and tunable material properties. However, with aging, these properties can change drastically, potentially leading to pathological solid-like states. Understanding the mechanisms behind these transitions is vital, yet remains elusive. Recent experiments have shed light on the aging processes of condensates, revealing a complex interplay of factors such as solvent depletion, strengthening of molecular interactions, and the formation of rigid structural segments. This study aims to delve deeper into these mechanisms to elucidate how they contribute to the aging dynamics and material properties of biomolecular condensates.

Main Objectives

- **Solvent Expulsion:** Examine how the removal of solvent from biomolecular condensates impacts their viscoelastic properties and contributes to the aging process.
- **Biopolymer Chain Rigidity:** Determine the role of biopolymer backbone rigidity in replicating the elastic behavior observed in aging condensates, comparing models with varying chain flexibilities.
- **Sticker Contact Lifetimes:** Analyze how the lifetimes of molecular interactions (sticker contacts) affect the transition of condensates from a viscous to a solid-like state, using both Maxwell fluid and Kelvin-Voigt models.
- **Simulate Non-Equilibrium Aging Dynamics:** Incorporate chain rigidification, desolvation, and sticker pair formation into a dynamic aging simulation to model the formation of solid shells around condensate surfaces, as reported in recent experimental findings.

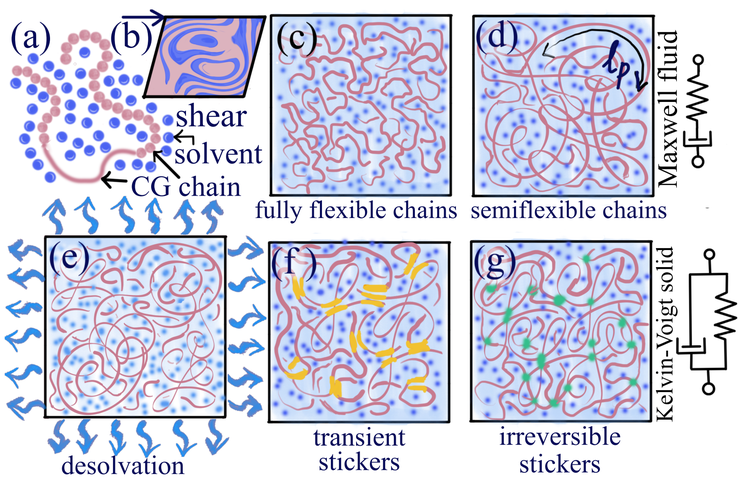

Figure 1: The schematic of models used to dissect the molecular driving forces of aging in biomolecular condensates. (a) A coarse-grained protein model with an explicit solvent is used to determine the rheological properties of condensates using (b) oscillatory shearing of the simulation box. (c) Fully flexible and (d) semiflexible chain models are used to analyze the role of chain rigidity on viscoelastic properties. (e) Solvent expulsion-driven shrinking is modeled in non-equilibrium simulations with (f) Short-lived thermoreversible sticker pairs and (g) Long-lived sticker pairs forming gel-like condensates

The role of chain rigidity and length

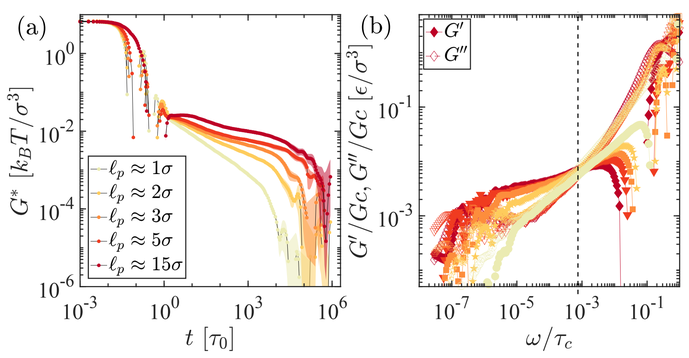

Figure 2: Viscoelastic responses as a function of rigidity of the polymer. (a) Complex modulus from the GK zero shear for different persistence lengths of the chains ranging from fully flexible $\ell_p \approx \sigma$ to stiffer chains $\ell_p \approx 15\sigma$. (b) The corresponding elastic and viscous moduli, G', G'' from the G^*.

The role of solvent expulsion

△ We fit the generalized Maxwell model $G = \sum_i G_i \exp(-t/\tau_i)$ with the complex modulus G^* data from the Green-Kubo method.

△ The crossover regime shifts an order of magnitudes in the ω range.

△ We fit the data with the generalized Maxwell model $G' = \sum_i G'_i \frac{\omega_i^2\tau_i^2}{1+\omega_i^2\tau_i^2}$, $G'' = \sum_i G''_i \frac{\omega_i\tau_i}{1+\omega_i^2\tau_i^2}$ to infer the $\omega \to 0$ limit response.

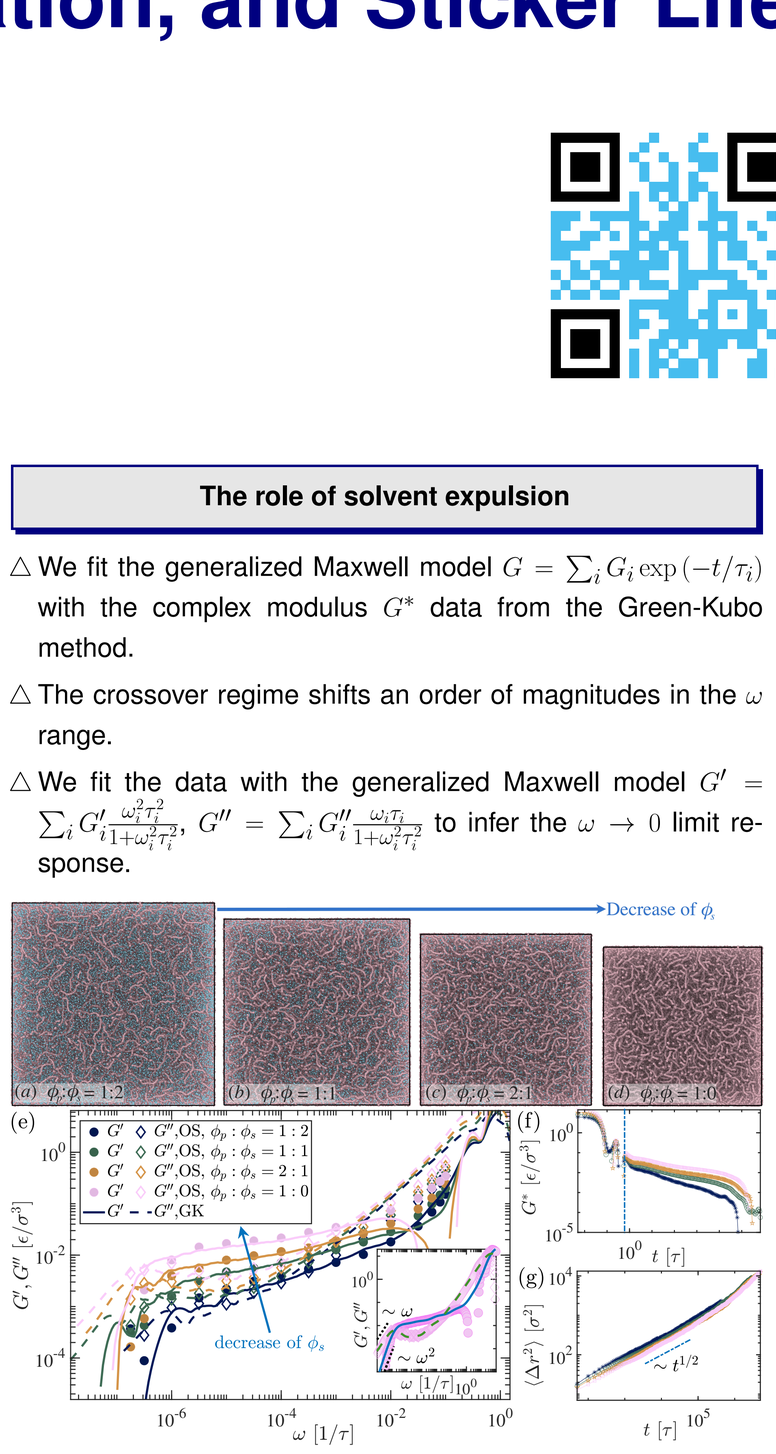

Figure 3: (a-d) Simulation snapshots depict polymer fraction ϕ_p (with fixed $\ell_p \approx 5\sigma$, pale chestnut color) and solvent (turquoise beads) fractions ϕ_s at various concentrations. (e) Viscoelastic properties, quantified by storage (G') and loss (G''), shown for different solvent fractions obtained using Green-Kubo (GK) and oscillatory shear (OS) methods. The inset of Fig. (e) displays the fitting of the generalized Maxwell model to G' and G'' from GK data for the scenario where $\phi_s = 0$. (f) The complex modulus (G^*) for four different concentrations was obtained using the GK method. The vertical dashed line separates the short and long time ranges, which are used to evaluate the Maxwell modes for longer timescales. (g) MSD of the chains behave subdiffusively as $\langle \Delta r^2 \rangle \sim t^{1/2}$.

Application to aging of FUS

♢ The coarse-grained HPS model of FUS protein [5, 6].

♢ A fully flexible FUS system is dominated by the viscous response throughout the frequency range.

♢ Adding an angular potential $\ell_p = 5\sigma$ becomes semiflexible FUS chains, which clearly shows the elastic modulus-dominated regions in Fig (4 b).

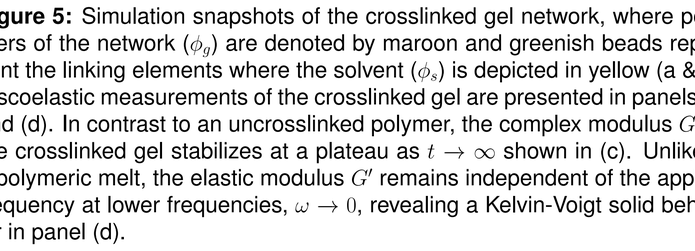

Figure 4: Total free energy, (a), as a function of the number of droplets N showing a minimum at $N_m \approx 23$ for $L = 200$. In the inset, Free energy of binary mixture is shown, where $N = 1$ is the lowest energy state. Surface energy F_s, increases, the elastic energy F_{el}, decreases, whereas, the bulk free energy $\mathcal{F}_b(\phi)$is almost independent of N as shown in (b). Panel (c) shows the dependence of the droplet radius R and the number density of the droplets n and the shear modulus of the gel G.

The limit of long sticker-sticker lifetimes

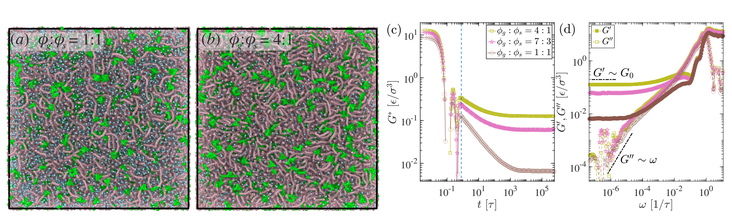

Figure 5: Simulation snapshots of the crosslinked gel network, where polymers of the network (ϕ_g) are denoted by maroon and greenish beads represent the linking elements where the solvent (ϕ_s) is depicted in yellow (a & b). Viscoelastic measurements of the crosslinked gel are presented in panels (c) and (d). In contrast to an uncrosslinked polymer, the complex modulus G^* of the crosslinked gel stabilizes at a plateau as $t \to \infty$ shown in (c). Unlike in a polymeric melt, the elastic modulus G' remains independent of the applied frequency at lower frequencies, $\omega \to 0$, revealing a Kelvin-Voigt solid behavior in panel (d).

Formation of corona shells during maturation

⊙ Spectroscopic observations reveal that a previously undetected population of FUS at the droplet surface gradually forms a solid shell, affecting protein exchange.

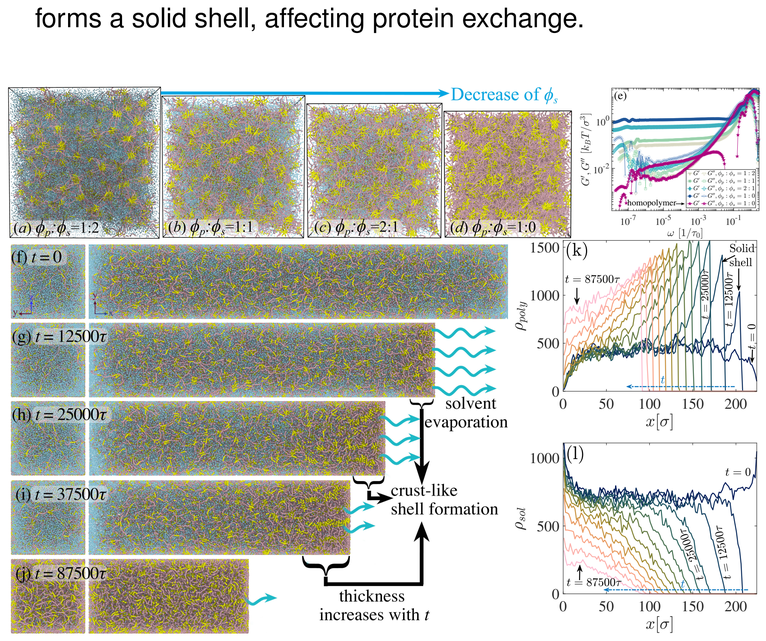

Figure 6: (a-d) Simulation snapshots depict the ratio of chains ϕ_p (represented by pale chestnut-colored strands and yellow stickers) as a function of the decrease in solvent concentration ϕ_s (depicted by turquoise beads). (e) Storage (G') and loss (G'') moduli for different concentrations of the sticky-rigid patch chains with varying ϕ_s. The homopolymer solution case from Fig. (3e) is included here as a reference for comparison. (f-j) Snapshots from non-equilibrium simulations of aging with evaporating solvent. Two perspective views of the simulation are shown: The left panel displays the squared surface perpendicular to the x direction (nonperiodic boundary) at $x(L(t))$ where evaporation takes place, while the right panel shows the elongated rectangular direction where the box length is shrinking, forming a crust-like shell at the boundary with time. (k) The number density of the polymer ρ_{poly} and (l) number density of the solvent ρ_{sol} in the box along the x direction as a function of time are also presented.

Summary

■ We have established that the interplay of solvent expulsion and chain rigidification is crucial in determining the onset of aging.

■ Due to desolvation, condensates become denser, and sticky segments come together, increasing the characteristic relaxation time and making it more elastic.

■ Viscoelasticity requires semiflexible HPS chains. The lifetime of sticker pairs profoundly influences the mature state of the condensates; short-lived stickers lead to a Maxwell fluid behavior [2].

■ The longer-lived, irreversibly crosslinked stickers result in solid-like properties, consistent with the Kelvin-Voigt model [3]

■ By varying chain rigidity, desolvation, and sticker pair formation, we demonstrate the mechanism forming solid-like shells around condensates, consistent with recent experiments [4].

References

[1] S. Biswas, & Davit A Potoyan, *PRX Life*, **2**, 023011, (2024).

[2] L. Jawerth, *et al.* Science 370, 1317 (2020).

[3] I. Alshareedah, *et al. Nat. Phys.*. **1-10**, 011028 (2024).

[4] L. Emmanouilidis *et al.*, *Nat Chem Bio.* **1–9**, (2024).

[5] G.L. Dignon, *et al. PLoS Comp. Bio.* **14(1)**, e1005941 (2018).

[6] A. R. Tejedor, *et al. J. Phys. Chem. B.* **127(20)**, 4441 (2023).

Acknowledgment

□ The authors acknowledge the support from the Research Corporation for Scientific Advancement Cottrell Scholar Award.

□ DP also acknowledges support from the National Institutes of Health with grant no R35GM138243.